

Promotion effect of intercalated citrate anion on the reconstruction of NiFe LDH for oxygen evolution reaction

Xiong He^{a}, Jiayang Cai^b, Qiyi Chen^a, Jinghua Liu^{a*}, Qijun Zhong^a, Jingyan Liu^c,
Zijun Sun^a, Dezhi Qu^b, Yao Lu^b, Xin Li^{c*}*

^a School of Electronic Engineering, Liuzhou Key Laboratory of New Energy Vehicle Power Lithium Battery, Guangxi Engineering Research Center for Characteristic Metallic Powder Materials, Guangxi University of Science and Technology, Liuzhou 545000, China.

^b Guangxi Key Laboratory of Green Processing of Sugar Resources, College of Biological and Chemical Engineering, Guangxi University of Science and Technology, Liuzhou 545006, China.

^c MIT Key Laboratory of Critical Materials Technology for New Energy Conversion and Storage, School of Chemistry and Chemical Engineering, State Key Lab of Urban Water Resource and Environment, Harbin Institute of Technology, Harbin 150090, China.

*Corresponding author: Tel.: +86-0451-86282153.

E-mail address: hexiong@gxust.edu.cn (X. He), liujinghua@gxust.edu.cn (J. Liu),

lixin@hit.edu.cn (X. Li)

Table of content

Fig. S1 (a) XRD patterns at the (003) and (b) XRD patterns at the (006) plane of these samples.

Fig. S2 (a-c) SEM images of NiFe LDH, (d-f) SEM images of NiFe LDH-CA2, and (g-i) SEM images of NiFe LDH-CA3.

Fig. S3 (a) N₂ adsorption/desorption isotherm and (b) pore size distribution curves of these samples.

Fig. S4 XPS survey of NiFe LDH and NiFe LDH-CA2.

Fig. S5 (a) LSV curves and (b) corresponding Tafel plots of Ni(OH)₂, Fe(OH)₃, and NiFe LDH-CA2.

Table S1 OER activity comparison with other NiFe based electrocatalysts

Fig. S6 CV curves of these samples in the region of 0.4-1.4 V vs. RHE.

Fig. S7 CV curves of (a) NiFe LDH, (b) NiFe LDH-CA1 and (c) NiFe LDH-CA3 with different scan rates.

Fig. S8 CP curve at 150 and 250 mA/cm² for NiFe LDH-CA2.

Fig. S9 Nyquist plots of these samples.

Fig. S10 CV curves of (a) NiFe LDH, (b) NiFe LDH-CA1, and (c) NiFe LDH-CA3.

Fig. S11 (a) LSV curves of these samples and (b) LSV curves of NiFe LDH with different CA addition in KOH electrolyte.

Fig. S12 Optical images of these samples before and after OER test.

Table S2. Elemental composition of electrocatalyst from XPS

Fig. S13 (a) FTIR spectra of NiFe LDH-CA2 before and after OER, and (b) Raman spectrum of NiFe LDH-CA2 after OER.

Fig. S14 LSV curves of NiFe LDH in KOH electrolyte with various CA additions.

Fig. S15 LSV curves of pristine NiFe LDH-CA2, washed NiFe LDH-CA2 in new KOH electrolyte, and washed NiFe LDH-CA2 in KOH electrolyte with 10 mM CA addition.

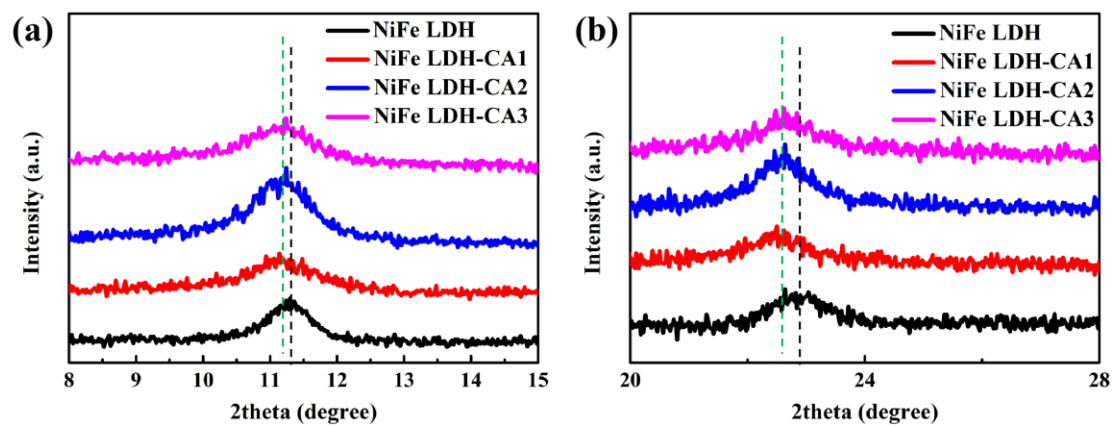


Fig. S1 (a) XRD patterns at the (003) and (b)XRD patterns at the (006) plane of these samples.

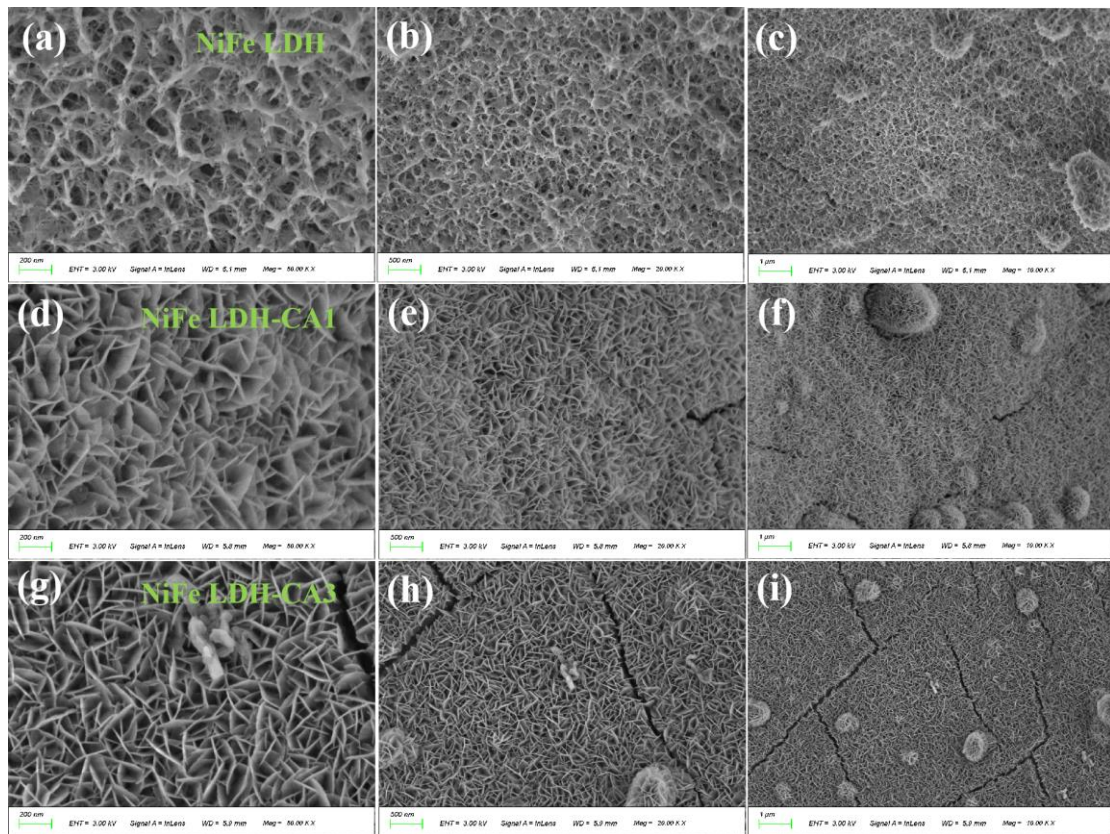


Fig. S2 (a-c) SEM images of NiFe LDH, (d-f) SEM images of NiFe LDH-CA2, and (g-i) SEM images of NiFe LDH-CA3.

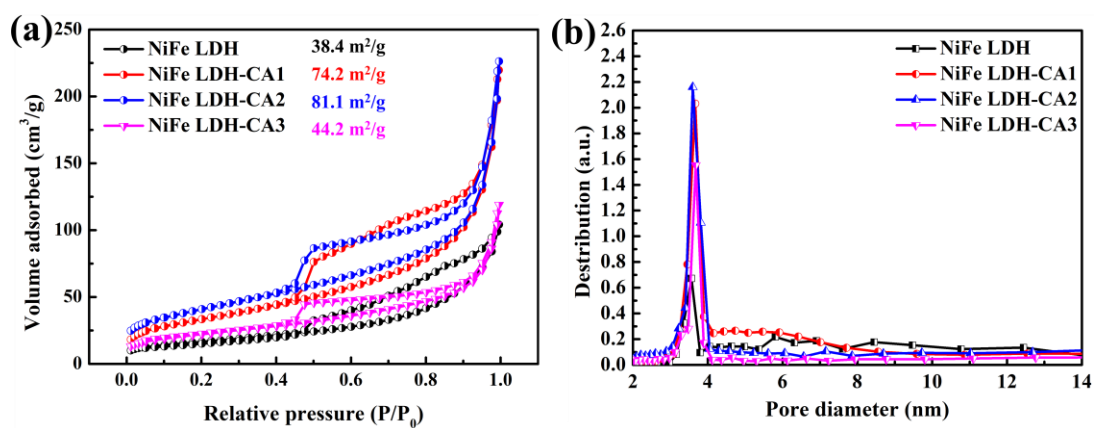


Fig. S3 (a) N_2 adsorption/desorption isotherm and (b) pore size distribution curves of these samples.

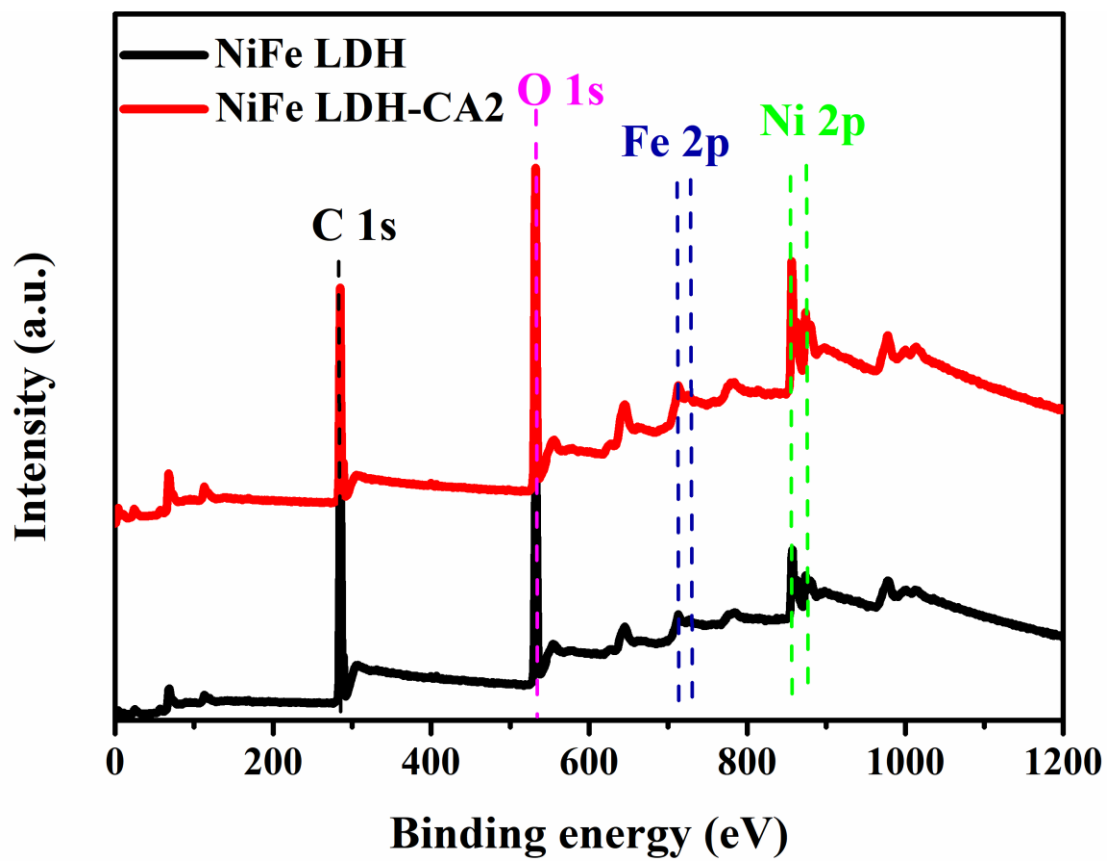


Fig. S4 XPS survey of NiFe LDH and NiFe LDH-CA2.

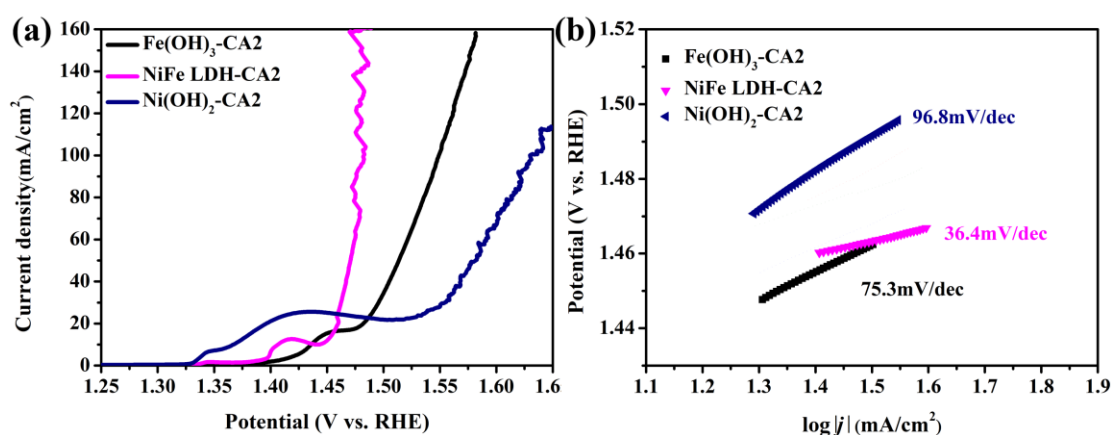


Fig. S5 (a) LSV curves and (b) corresponding Tafel plots of Ni(OH)₂, Fe(OH)₃, and NiFe LDH-CA2.

Table S1 OER activity comparison with other NiFe based electrocatalysts

Electrocatalysts	Overpotential	Tafel slope	Year	Reference
NiFe LDH-CA2	242 mV at 50 mA/cm²	36.4 mV/dec	2023	This work
FeNi-HDNAs	274 mV at 50 mA/cm ²	91.66 mV/dec	2020	[1]
FeNiP/C-900	229 mV at 10 mA/cm ²	74.5 mV/dec	2019	[2]
FeNi _{4.34} @FeNi-Foil	283 mV at 10 mA/cm ²	53 mV/dec	2017	[3]
NiFe-NiCoO ₂	286 mV at 10 mA/cm ²	49.3 mV/dec	2019	[4]
NiFeMoO	270 mV at 50 mA/cm ²	66.6 mV/dec	2020	[5]
NiFe-POMo	255 mV at 10 mA/cm ²	43.8 mV/dec	2021	[6]
FeNi-MOF/CFA/NiMoO ₄	256 mV at 10 mA/cm ²	68.9 mV/dec	2022	[7]
Mo _{0.5} PS NiFe LDH	259 mV at 10 mA/cm ²	62 mV/dec	2020	[8]
NiFe LDH-TEA	261 mV at 10 mA/cm ²	32.5 mV/dec	2022	[9]
NiFe(20Ni) MOF/NFF	226 mV at 10 mA/cm ²	87.1 mV/dec	2022	[10]
NC-PB@CNT	240 mV at 10 mA/cm ²	73 mV/dec	2021	[11]

Note: HDNAs is hydroxides nanotube arrays; LDH is layered double hydroxide; MOF is metal-organic framework; CFA is caffeic acid; TEA is triethanolamine; NFF is nickel-iron foam, NC-PB is Ni-Co hexacyano nano-frameworks, CNT is carbon nanotubes.

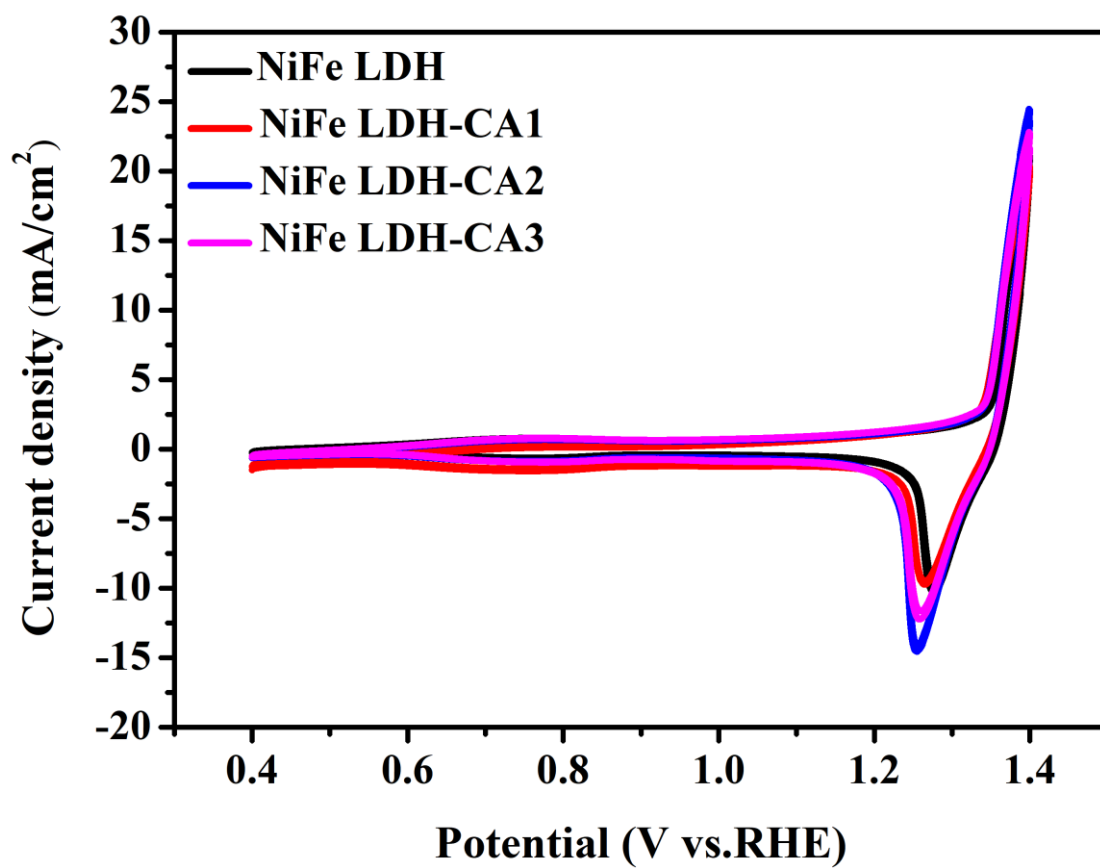


Fig. S6 CV curves of these samples in the region of 0.4-1.4 V vs. RHE.

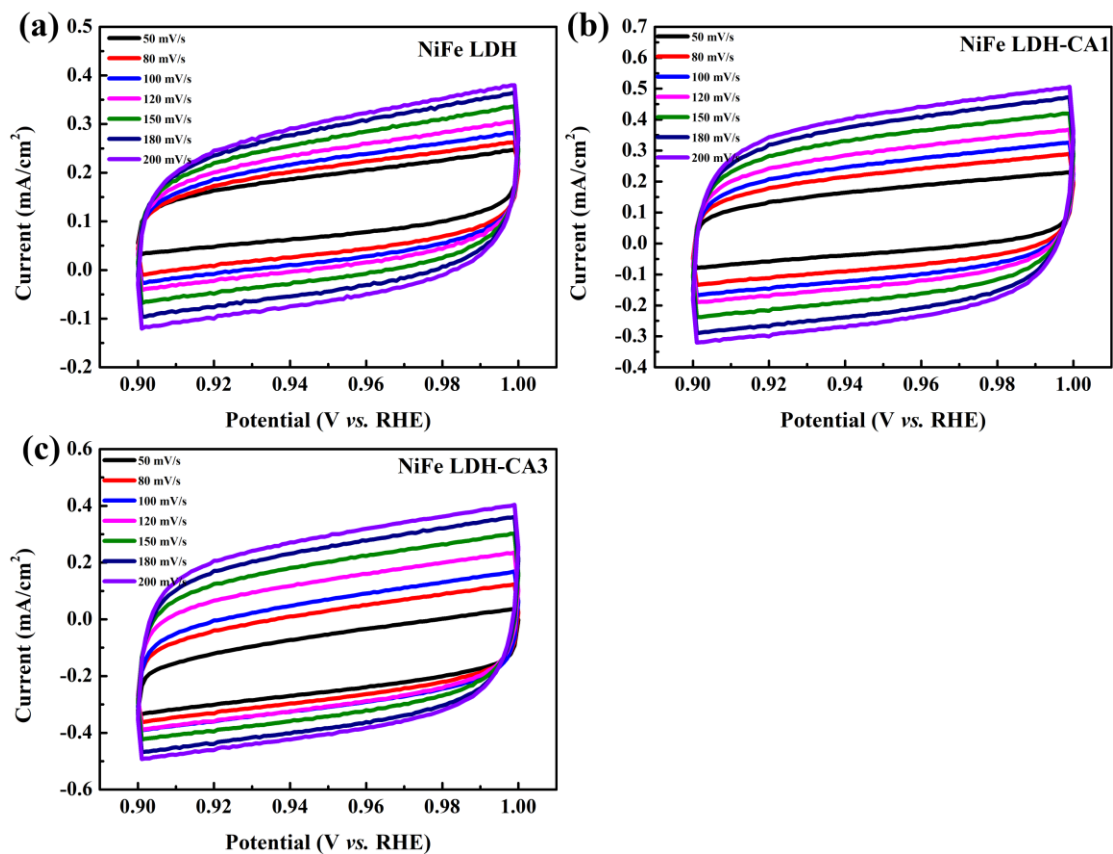


Fig. S7 CV curves of (a) NiFe LDH, (b) NiFe LDH-CA1 and (c) NiFe LDH-CA3 with different scan rates.

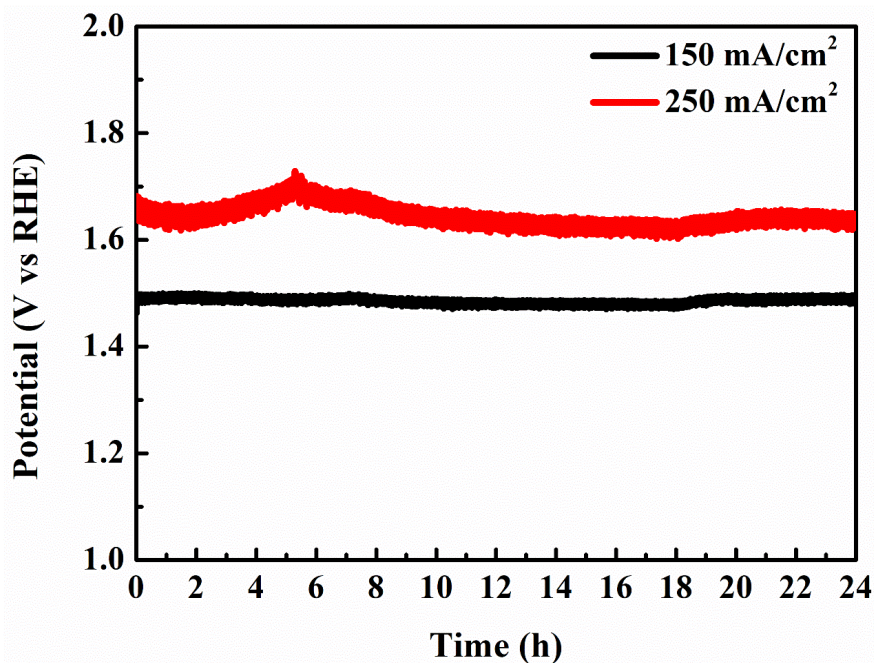


Fig. S8 CP curve at 150 and 250 mA/cm² for NiFe LDH-CA2.

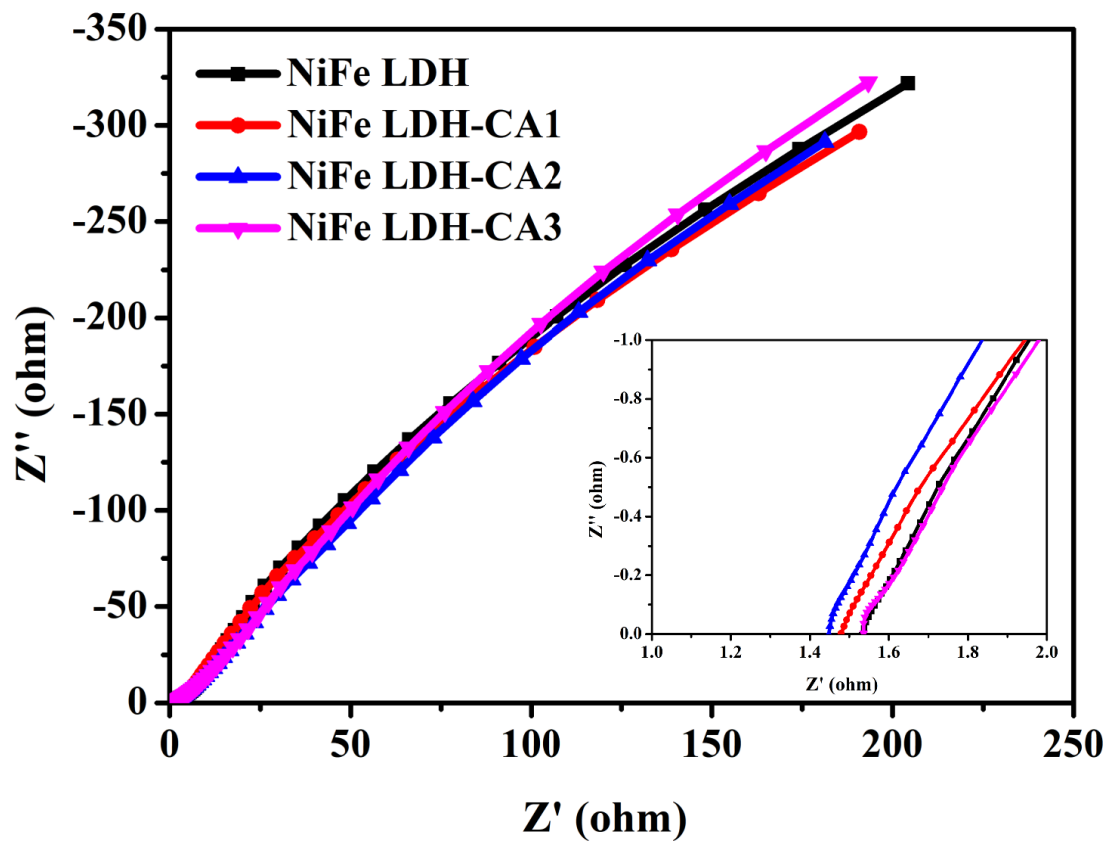


Fig. S9 Nyquist plots of these samples.

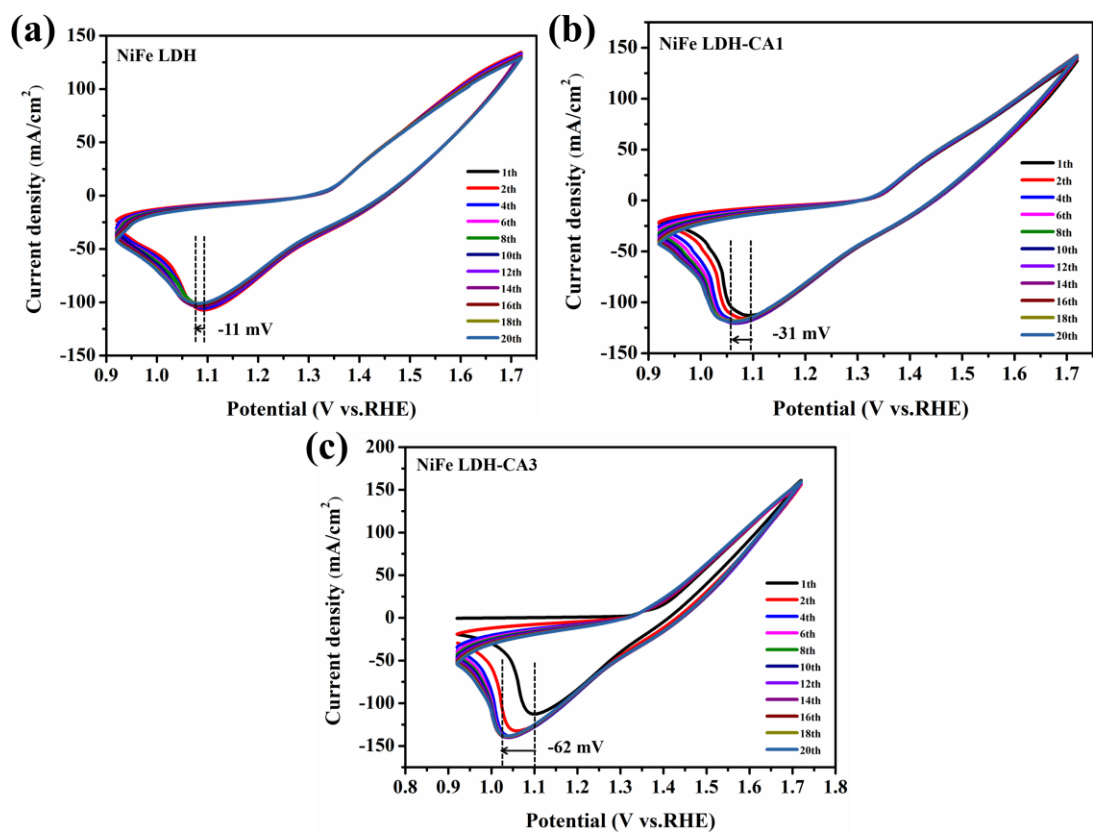


Fig. S10 CV curves of (a) NiFe LDH, (b) NiFe LDH-CA1, and (c) NiFe LDH-CA3.

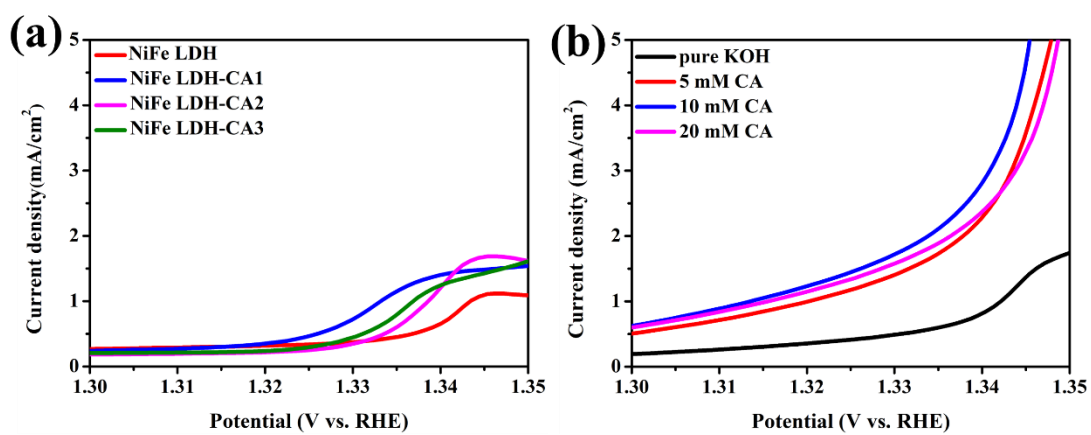


Fig. S11 (a) LSV curves of these samples and (b) LSV curves of NiFe LDH with different CA addition in KOH electrolyte.

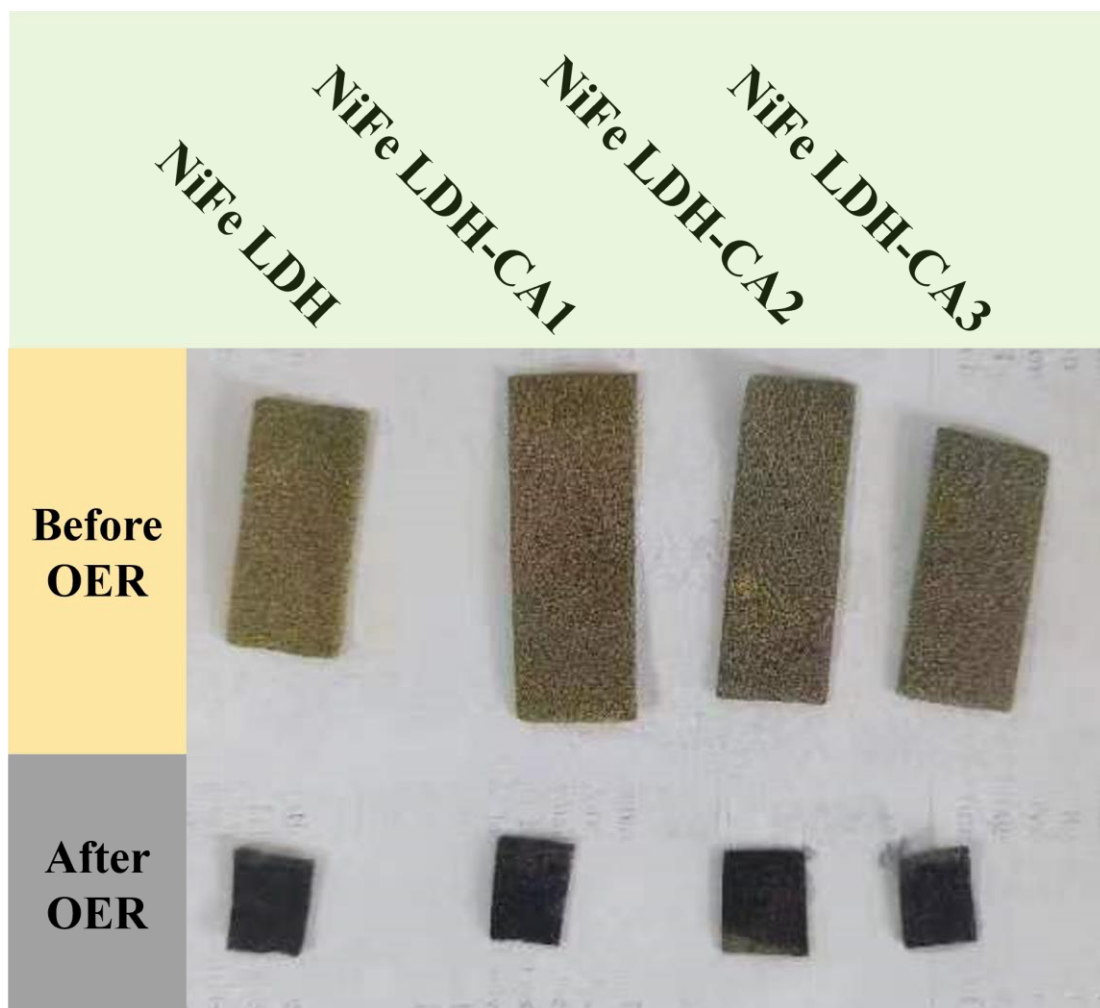


Fig. S12 Optical images of these samples before and after OER test.

Table S2. Elemental composition of electrocatalyst from XPS

Samples	C (%)	Fe (%)	Ni (%)	O (%)
NiFe LDH	64.53	1.18	2.89	31.41
NiFe LDH-CA2	54.33	2.77	5.77	37.13
NiFe LDH-CA2 after OER	41.34	4.78	13.90	39.98

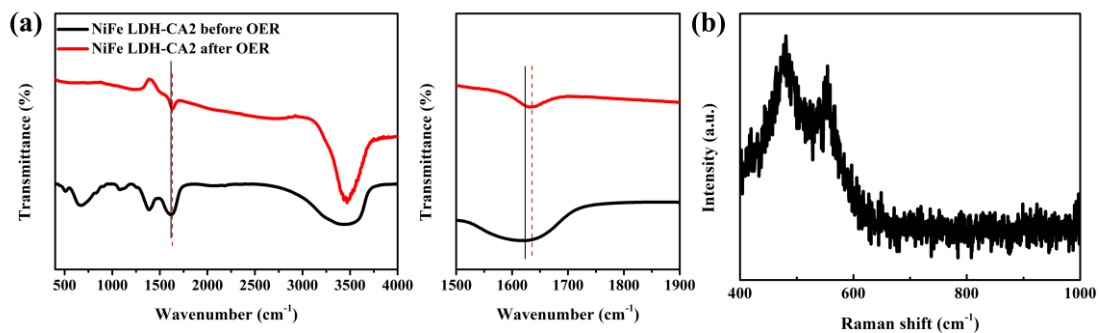


Fig. S13 (a) FTIR spectra of NiFe LDH-CA2 before and after OER, and (b) Raman spectrum of NiFe LDH-CA2 after OER.

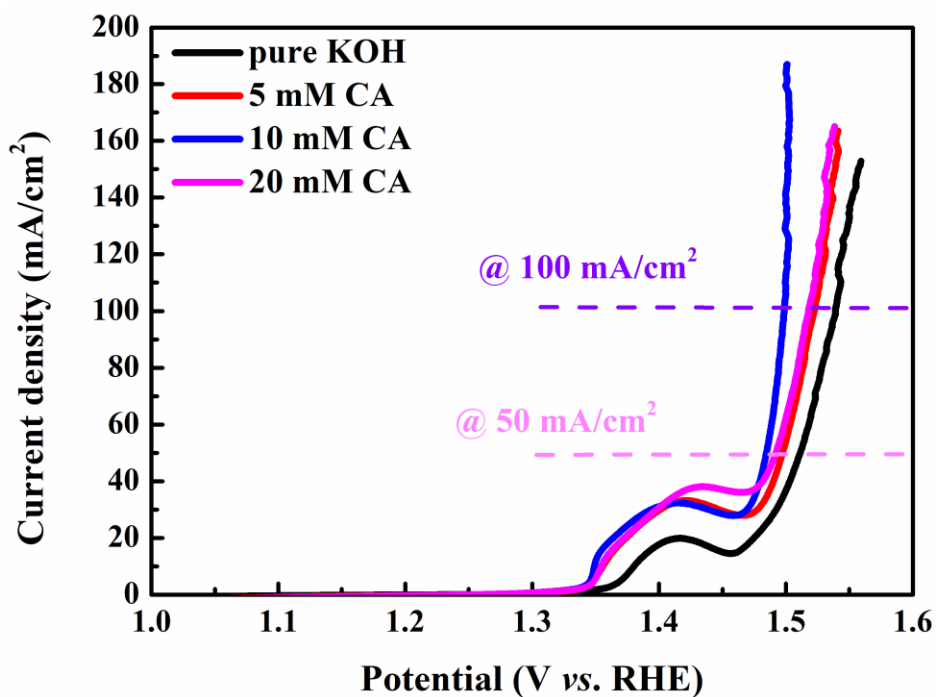


Fig. S14 LSV curves of NiFe LDH in KOH electrolyte with various CA additions.

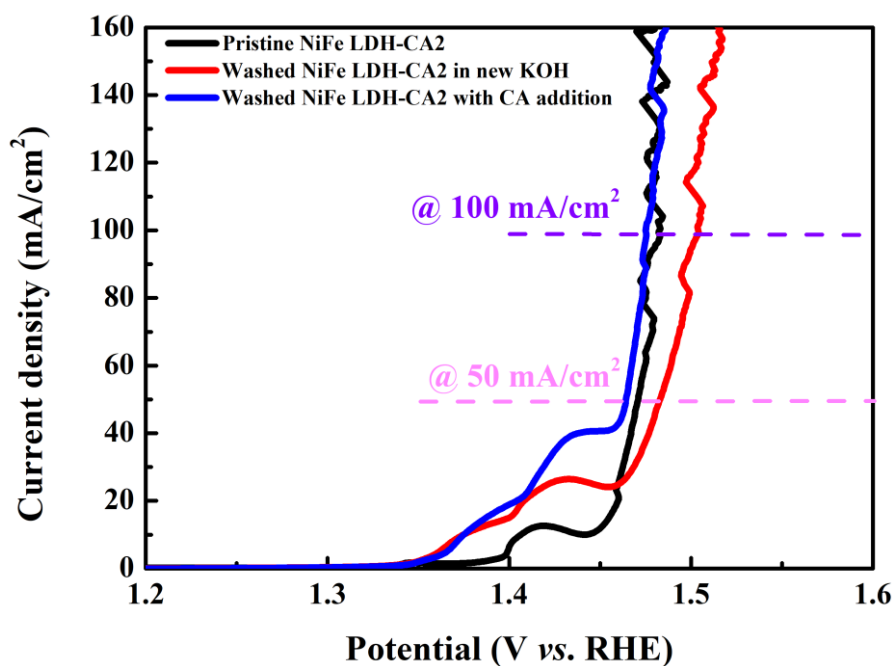


Fig. S15 LSV curves of pristine NiFe LDH-CA2, washed NiFe LDH-CA2 in new KOH electrolyte, and washed NiFe LDH-CA2 in KOH electrolyte with 10 mM CA addition.

Reference

- [1] N. Yu, W. Cao, M. Huttula, Y. Kayser, P. Hoenicke, B. Beckhoff, F. Lai, R. Dong, H. Sun, B. Geng, Fabrication of FeNi hydroxides double-shell nanotube arrays with enhanced performance for oxygen evolution reaction, *Applied Catalysis B: Environmental*, 261 (2020) 118193.
- [2] X. Wang, L.L. Chai, J.Y. Ding, L. Zhong, Y.J. Du, T.T. Li, Y. Hu, J.J. Qian, S.M. Huang, Chemical and morphological transformation of MOF-derived bimetallic phosphide for efficient oxygen evolution, *Nano Energy*, 62 (2019) 745-753.
- [3] U.Y. Qazi, C.-Z. Yuan, N. Ullah, Y.-F. Jiang, M. Imran, A. Zeb, S.-J. Zhao, R. Javaid, A.-W. Xu, One-Step Growth of Iron–Nickel Bimetallic Nanoparticles on FeNi Alloy Foils: Highly Efficient Advanced Electrodes for the Oxygen Evolution Reaction, *ACS Applied Materials & Interfaces*, 9 (2017) 28627-28634.
- [4] R. Shi, J. Wang, Z. Wang, T. Li, Y.-F. Song, Unique NiFeNiCoO₂ hollow polyhedron as bifunctional electrocatalysts for water splitting, *Journal of Energy Chemistry*, 33 (2019) 74-80.
- [5] Y. Wang, Y. Zhu, S. Zhao, S. She, C. Selomulya, Anion Etching for Accessing Rapid and Deep Self-Reconstruction of Precatalysts for Water Oxidation, *Matter*, (2020).
- [6] X. Liu, F. Xia, R. Guo, M. Huang, J. Meng, J. Wu, L. Mai, Ligand and Anion Co-Leaching Induced Complete Reconstruction of Polyoxomolybdate–Organic Complex Oxygen-Evolving Pre-Catalysts, *Advanced Functional Materials*.
- [7] Y. He, F. Yan, B. Geng, C. Zhu, X. Zhang, X. Zhang, Y. Chen, Metal-organic framework interface engineering for highly efficient oxygen evolution reaction, *Journal of Colloid and Interface Science*, 619 (2022) 148-157.
- [8] Y.-Y. Dong, D.-D. Ma, X.-T. Wu, Q.-L. Zhu, Electron-withdrawing anion intercalation and surface

sulfurization of NiFe-layered double hydroxide nanoflowers enabling superior oxygen evolution performance, *Inorganic Chemistry Frontiers*, 7 (2020) 270-276.

[9] Y. Zheng, H. Deng, H. Feng, G. Luo, R. Tu, L. Zhang, Triethanolamine-assisted synthesis of NiFe layered double hydroxide ultrathin nanosheets for efficient oxygen evolution reaction, *Journal of Colloid and Interface Science*, 629 (2023) 610-619.

[10] J. Wang, Y. Jiang, C. Liu, Y. Wu, B. Liu, W. Jiang, H. Li, G. Che, In situ growth of hierarchical bimetal-organic frameworks on nickel-iron foam as robust electrodes for the electrocatalytic oxygen evolution reaction, *Journal of Colloid and Interface Science*, 614 (2022) 532-537.

[11] S.A. Patil, S. Cho, Y. Jo, N.K. Shrestha, H. Kim, H. Im, Bimetallic Ni-Co@hexacyano nano-frameworks anchored on carbon nanotubes for highly efficient overall water splitting and urea decontamination, *Chemical Engineering Journal*, 426 (2021) 130773.